The Journal of Infectious Diseases

MAJOR ARTICLE

Escape From Monoclonal Antibody Neutralization Affects Henipavirus Fitness In Vitro and In Vivo

Viktoriya Borisevich,[1,3] Benhur Lee,[6] Andrew Hickey,[7] Blair DeBuysscher,[5] Christopher C. Broder,[7] Heinz Feldmann,[5] and Barry Rockx[1,2,3,4,5,8]

[1]Department of Pathology, [2]Department of Microbiology and Immunology, [3]Institute for Human Infections and Immunity, and [4]Sealy Center for Vaccine Development, University of Texas Medical Branch, Galveston; [5]Laboratory of Virology, Division of Intramural Research, National Institute of Allergy and Infectious Diseases, National Institutes of Health, Hamilton, Montana; [6]Department of Microbiology, Icahn School of Medicine at Mount Sinai, New York, New York; [7]Department of Microbiology and Immunology, Uniformed Services University, Bethesda, Maryland; and [8]Department of Rare and Emerging Viral Infections and Response, Center for Infectious Disease Control, National Institute of Public Health and the Environment, Bilthoven, The Netherlands

Henipaviruses are zoonotic viruses that can cause severe and acute respiratory diseases and encephalitis in humans. To date, no vaccine or treatments are approved for human use. The presence of neutralizing antibodies is a strong correlate of protection against lethal disease in animals. However, since RNA viruses are prone to high mutation rates, the possibility that these viruses will escape neutralization remains a potential concern. In the present study, we generated neutralization-escape mutants, using 6 different monoclonal antibodies, and studied the effect of these neutralization-escape mutations on in vitro and in vivo fitness. These data provide a mechanism for overcoming neutralization escape by use of cocktails of cross-neutralizing monoclonal antibodies that recognize residues within the glycoprotein that are important for virus replication and virulence.

Keywords. henipavirus; neutralizing antibody; monoclonal antibody; neutralization escape.

Henipaviruses (HNVs) are emerging zoonotic viruses that belong to the family *Paramyxoviridae* [1]. The genus *Henipavirus* is currently composed of 3 viruses, Hendra virus (HeV), Nipah virus (NiV), and Cedar virus [2]. Outbreaks of HeV and NiV infection occur almost yearly in horses and/or humans, and the human case-fatality rates range from 57%–100% [1]. Currently, no vaccines or therapeutics are approved for use in humans. Neutralizing antibodies are a strong correlate of protection in experimental animal challenge models [3–7]. A well-characterized human neutralizing monoclonal antibody (m102.4) has been used on a compassionate-use basis in 9 individuals who were at high risk of exposure to HeV in Australia and in 1 individual at high risk of exposure to NiV in the United States [8]. Several neutralizing monoclonal antibodies (mAbs) have been described that target the HNV glycoprotein (G) [8–10]. G is a type II transmembrane glycoprotein with a N-terminal cytoplasmic tail, a transmembrane domain, and a C-terminal ectodomain, which is divided into the stalk region and the globular head domain. The globular head domain is involved in receptor binding, while the stalk region is involved in triggering the fusion protein (F) to induce virus-cell fusion [11]. The 2 main mechanisms of neutralization involve blocking the interaction of the HNV G with its receptors ephrin B2 and B3, to block virus attachment or blocking the induction of fusion. Recently, the crystal structure of HeV G bound to a derivative of the human mAb m102.4 was solved [12], showing that the interaction of m102.4 involves binding of 4 hydrophobic pockets that also engage the HNV receptors, suggesting direct competition for the receptor-binding site [12].

These data show that neutralizing mAbs are promising candidates for prophylactic prevention and treatment of HNV infection. However, the high mutation rates associated with RNA virus replication also increase concerns about mutations that confer escape from neutralization. Therefore, it is important to understand the mechanisms of neutralization escape and the potential impact on viral fitness.

Here we identified and characterized several neutralization-escape mutations generated in vitro with a panel of human and mouse mAbs and assessed their impact on virulence in the well-established lethal hamster model.

MATERIALS AND METHODS

Ethics Statement

Approval for animal experiments was obtained from the University of Texas Medical Branch Institutional Animal Care and Use Committee. Animal work was performed by certified staff in an Association for Assessment and Accreditation of Laboratory Animal Care–approved facility. Animal housing, care, and experimental protocols were in accordance with National Institutes of Health guidelines.

Viruses

HeV, NiV strain Malaysia (NIV-M), and NiV strain Bangladesh (NiV-B) were kindly provided by the Special Pathogens Branch (Centers for Disease Control and Prevention, Atlanta, Georgia). The viruses were propagated on Vero cells (CCL-81; ATCC) as described previously [13].

Received 5 June 2015; accepted 1 September 2015; published online 10 September 2015.

Correspondence: B. Rockx, Department of Rare and Emerging Viral Infections and Response, Centre for Infectious Disease Control, National Institute for Public Health and the Environment, PO Box 1, 3720 BA Bilthoven, The Netherlands (barry.rockx@rivm.nl).

The Journal of Infectious Diseases® 2016;213:448–55

DOI: 10.1093/infdis/jiv449

Monoclonal Antibodies and Escape Mutants

A panel of 6 HNV G–specific mAbs were used in this study. mAbs against HNVs were generated as described previously [9, 14]. Mouse mAbs nAH1.3 and 213 were generated against NiV-M, while mouse mAbs hAH14.2, hAH1.3, and hAH5.1 and human mAb m102.4 were generated against HeV. Neutralization-resistant NiV-M and HeV mutants were generated as described previously [12].

Neutralization Assay

Neutralizing titers were determined by a plaque reduction neutralization titer (PRNT) assay. For the PRNT, mAbs were serially diluted 2-fold and incubated with 100 plaque-forming units (PFU) of NiV-M, NiV-B, or HeV for 1 hour at 37°C. The virus and antibody mixture was then added to a 6-well plate with 5×10^5 Vero cells/well in triplicate. After incubation for 1 hour at 37°C, cells were overlaid with 3 mL of 0.8% agarose in medium. Plates were incubated for 3 days at 37°C and stained with crystal violet in 10% formalin, and plaques were counted. The percentage of neutralization was calculated as [1 − (number of plaques with antibody/number of plaques without antibody)] × 100. All assays were performed in triplicate.

Structural Mapping of Neutralization-Escape Mutations

The crystal structure coordinates of the HeV and NiV-M attachment proteins G interacting with their receptor the human Ephrin B2 (PDB code 2VSK and 2VSM2, respectively) were used to determine the locations of amino acid residues associated with neutralization escape [15]. All molecular representations were produced with PyMOL (Delano Scientific).

Virus Growth Curves

Growth curves were performed by inoculating Vero cell cultures with NiV-M, HeV, and their escape mutants at a low multiplicity of infection (MOI) of 0.01 for 1 hour, after which the cells were washed 3 times with phosphate-buffered saline and overlaid with medium. Virus samples were obtained at various time points after infection and stored at −80°C until viral titers were determined by a 50% tissue infective culture dose ($TCID_{50}$) assay, as previously described [16].

Animal Studies

Female Syrian golden hamsters (*Mesocricetus auratus*; 6-week-old HsdHan:AURA hamsters from Harlan Laboratories) were inoculated with 10^5 $TCID_{50}$ of HeV, NiV-M, or their respective neutralization-escape mutants in a 100-µL volume via the intraperitoneal route and were monitored as described previously [16]. For the pathogenesis study, groups of 5 animals were euthanized on day 3 after infection or when moribund, and whole-blood samples (collected in Vacutainer tubes containing ethylenediaminetetraacetic acid), as well as spleen, kidney, lung, and brain, were removed for virus isolation. Virus titration of tissue samples was performed as described previously [16].

RESULTS

Identification of Amino Acids That Are Critical for HNV Neutralization

mAbs hAH14.2 and hAH1.3 were used for selection of neutralization-escape mutants of HeV, mAbs nAH1.3, hAH5.1 and 213 were used for selection of neutralization-escape mutants of NiV-M, and mAb m102.4 was previously used to generate a neutralization-escape mutant of both HeV and NiV-M [12].

Five of 7 escape mutants contained a single amino acid change in G, while escape mutants generated by using mAbs hAH5.1 and 213 resulted in 2 amino acid changes each in G (Supplemental Table 1). We previously showed that the m102.4 escape mutants resulted in an amino acid change in NiV-M G at position V507I and in HeV G at position D582N [12]. The nAH1.3 escape mutant contained a single amino acid change at position Q450K in NiV-M G. Interestingly, both mAb hAH5.1 and 213 neutralization-escape mutants contained an amino acid change at position N159D. In addition to this N159D change, the hAH5.1 neutralization-escape mutant contained a mutation at position R516K, whereas the mAb 213 mutant contained a mutation at Q388R. In HeV G, an amino acid change was present at position H406Y in the hAH14.2 escape mutant. Finally, generation of neutralization-escape mutants by using the mAb hAH1.3 resulted in an amino acid change at position S134F in HeV G.

Cross-neutralization of Escape Mutants

Unfortunately, hybridomas producing mAbs hAH5.1 and hAH14.2 used in generating escape mutants were lost owing to a technical failure during storage. Thus, all further analyses were performed with mAbs m102.4, nAH1.3, 213, and hAH1.3.

First, the neutralizing antibody titers for each of the mAbs against HeV, NiV-M, and NiV-B were determined (Figure 1). mAbs m102.4 and nAH1.3 were able to neutralize HeV and both NiV-M and NiV-B efficiently (Figure 1*A* and 1*B*). mAb 213 neutralized NiV-M but not NiV-B or HeV (Figure 1*C*). mAb hAH1.3 efficiently neutralized HeV but none of the 2 NiV strains (Figure 1*D*).

Second, we determined whether other mAbs could still neutralize the escape mutants described above (Figures 2 and 3). Neutralization by mAb m102.4 was only affected by its respective escape mutations at V507I (NiV-M) and D582N (HeV; Figures 2*A* and 3*A*) and not by mutations generated by other mAbs. Neutralization by mAb nAH1.3 was affected by its respective NiV-M escape mutant at position Q450K but also by the mutations at N159D and R516K (Figure 2*B*), originally generated by mAb hAH5.1. Interestingly, the mutation at N159D in combination with a Q388R change did not affect neutralization, further suggesting that the N159D mutation is not involved in escape from neutralization. In addition, while mAb nAH1.3 was generated against NiV G, this antibody also potently neutralized HeV. Several mutations in HeV G were associated with a decrease in neutralization by mAb nAH1.3, including mutations at positions S134F, H406Y, and D582N (Figure 3*B*). For mAb

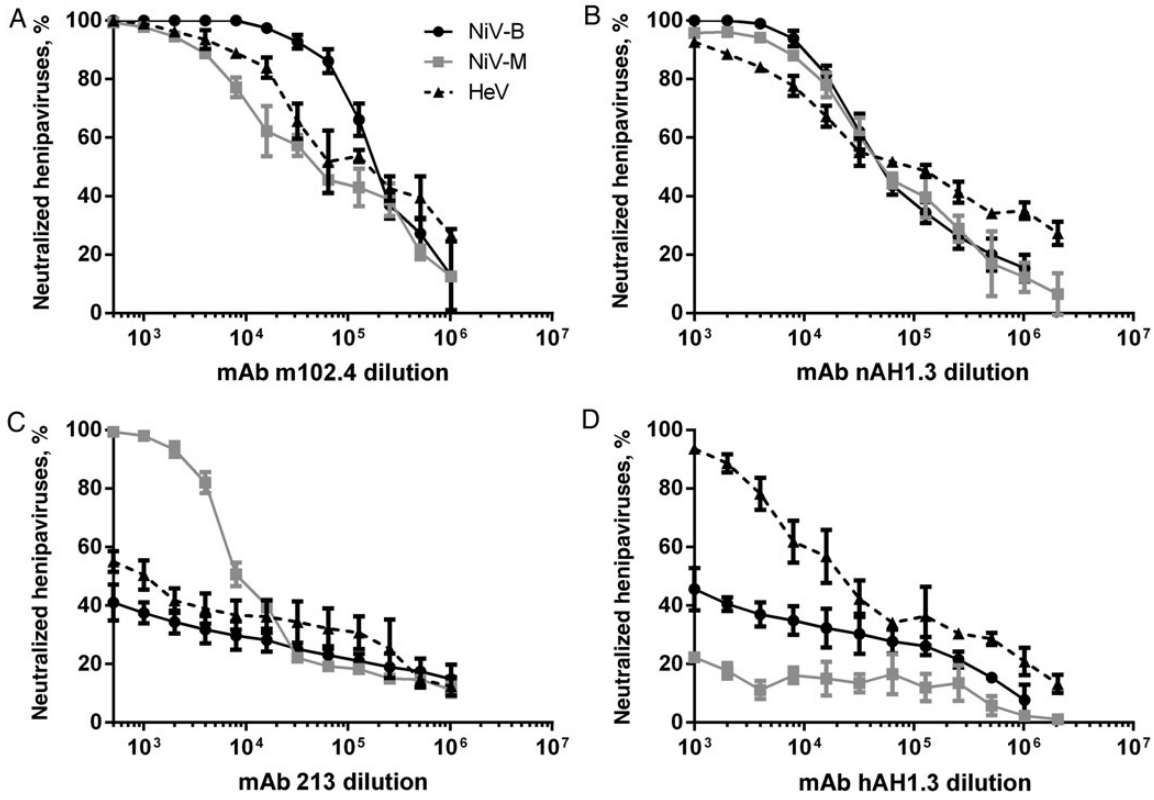

Figure 1. Neutralization of wild-type henipavirus strains. The neutralization of henipaviruses by monoclonal antibodies (mAbs) m102.4 (*A*), nAH1.3 (*B*), 213 (*C*), and hAH1.3 (*D*) was determined by a plaque reduction neutralization assay. Two Nipah virus (NiV) strains (Malaysia [NiV-M] and Bangladesh [NiV-B]) and 1 Hendra virus (HeV) strain were used. Neutralization was performed in triplicate and error bars represent the standard deviation.

213, neutralization was not only affected by the virus strain (Figure 1*C*) but also by its respective escape mutations N159D and Q388R (Figure 2*C*). Again, the N159D mutation in combination with an R516K change did not result in loss of neutralization. Finally, neutralization by hAH1.3 was affected by 3 mutations in HeV G, at positions S134F, H406Y, and D582N, similar to nAH1.3 (Figure 3*C*).

Structural Mapping of Amino Acids Critical for Neutralization

To better understand the mechanism of neutralization, the location of the amino acid changes associated with neutralization escape were mapped on the structure of the NiV and HeV G. Unfortunately, a structure of the stalk region of HeV G (residues 71–188) is not available, and therefore, we were unable to map the mutation at residue S134. The mutation at residue H406Y, associated with escape from neutralization by mAb nAH.3, is located near one of the 4 binding pockets that interact with residue W122 of ephrin B2 [17] and includes V401 and N402 on HeV G (Figure 4*A*). The mutation at D582N is next to residue Y581, which is part of the binding pocket for the ephrin B2 residue F117 (Figure 4*A*) [17]. The close proximities of these escape mutations to binding pockets suggest that the mAbs m102.4 and nAH1.3 and hAH1.3 all neutralize HeV by interfering with receptor binding.

Two of the mutations associated with escape from neutralization of NiV-M (V507I and Q388R) were previously shown to be important for forming and stabilizing the NiV-M G/ephrin complex [17, 18]. Residue V507 on the NiV-M G is involved in van der Waals interactions with residue P122 on ephrin B2 as part of one of the 4 receptor-binding pockets (Figure 4*B*) [18], whereas residue Q388 of NiV-M G is part of an intricate side-chain/side-chain hydrogen bond network that interacts with residue D108 on ephrin B2 (Figure 4*B*) [17]. Therefore, mAb m102.4 and mAb 213 target the receptor-binding domain, resulting in a direct blockade of the interaction of NiV-M with its receptors ephrin B2 and B3 as their likely mechanisms of neutralization. The mutations Q450K and R516K associated with escape of NiV-M from neutralization by mAb nAH1.3 are located next to each other at the bottom face of the globular head of NiV-M G, near the stalk domain (Figure 4*B*). Since this area is not known to interact with the receptors ephrin B2 or B3, the mechanism of action remains unknown.

Effect of G Mutations on In Vitro Replication

Since several of the neutralization-escape mutations were located in or near the receptor-binding site, we determined whether these mutations would affect the fitness of these escape mutants in vitro. The plaque morphology of the wild-type (WT) and

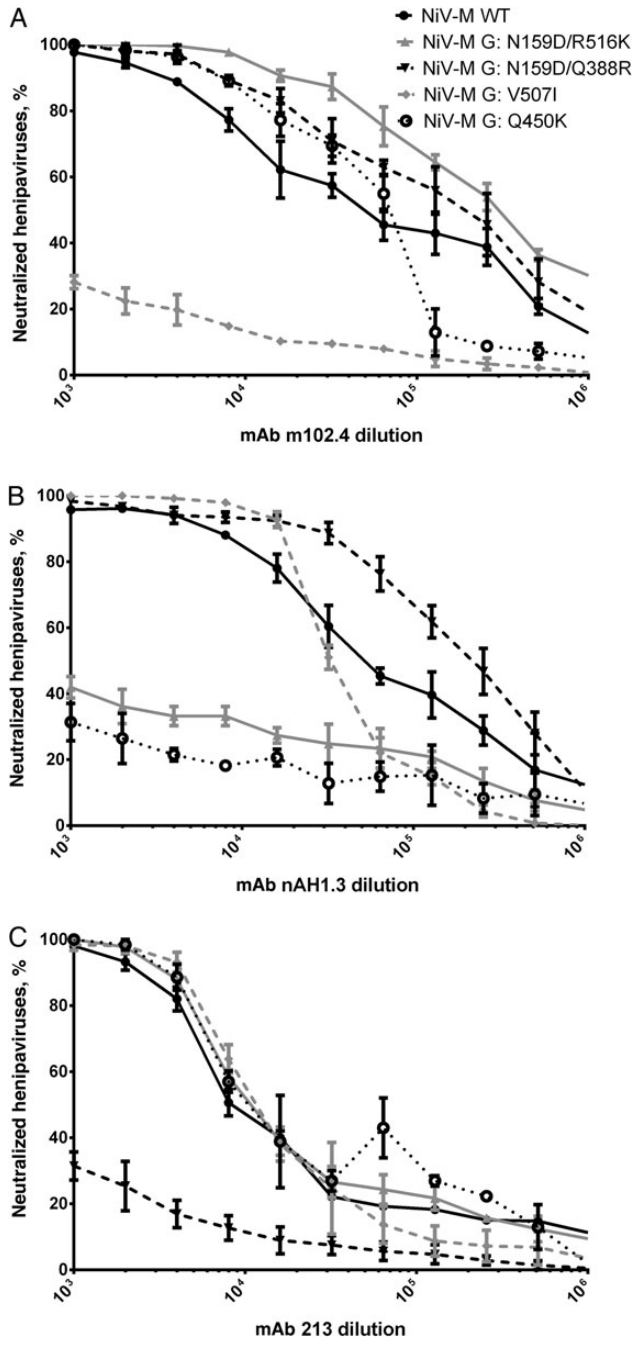

Figure 2. Cross-neutralization of Nipah virus (NiV) escape mutants. The neutralization of NiV strain Malaysia (NiV-M) escape mutants by monoclonal antibodies (mAbs) m102.4 (*A*), nAH1.3 (*B*), and 213 (*C*) was determined by a plaque reduction neutralization assay. Neutralization was performed in triplicate, and error bars represent standard deviations. Abbreviation: WT, wild type.

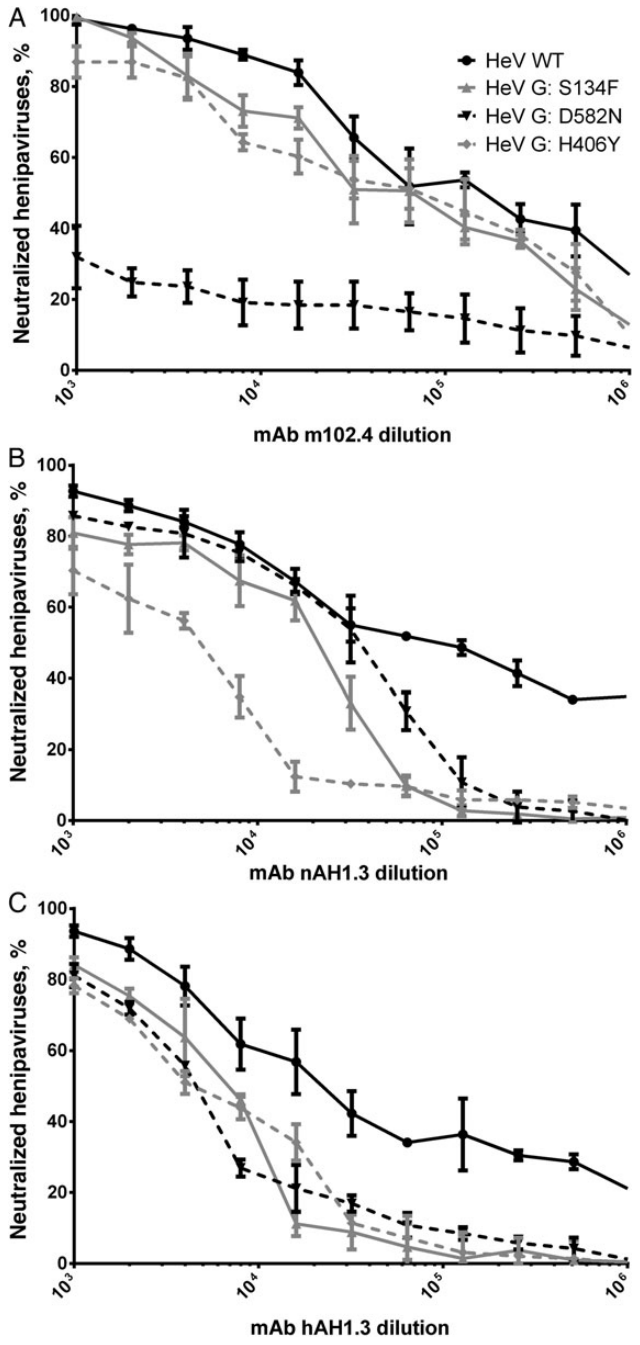

Figure 3. Cross-neutralization of Hendra virus (HeV) escape mutants. The neutralization of HeV escape mutants by monoclonal antibodies (mAbs) m102.4 (*A*), nAH1.3 (*B*), and hAH1.3 (*C*) was determined by a plaque reduction neutralization assay. Neutralization was performed in triplicate, and error bars represent standard deviations. Abbreviation: WT, wild type.

neutralization-escape mutants was very similar (data not shown). All HeV escape mutants grew to similar peak titers and with similar kinetics in Vero cells, compared with the WT HeV strain (Figure 5*A*). Similarly, all of the NiV-M–derived escape mutants grew to the same peak titers by 48 hours after infection. However, the escape mutant containing the N159D/R516K mutations was significantly delayed in replication at 18 hours after infection, compared with the WT strain (Figure 5*B*).

Effect of G Mutations on In Vivo Virulence and Replication

Since in vitro replication does not always correlate with in vivo virulence, we next determined the virulence of the escape mutants in hamsters. For HeV, mutations in G, associated

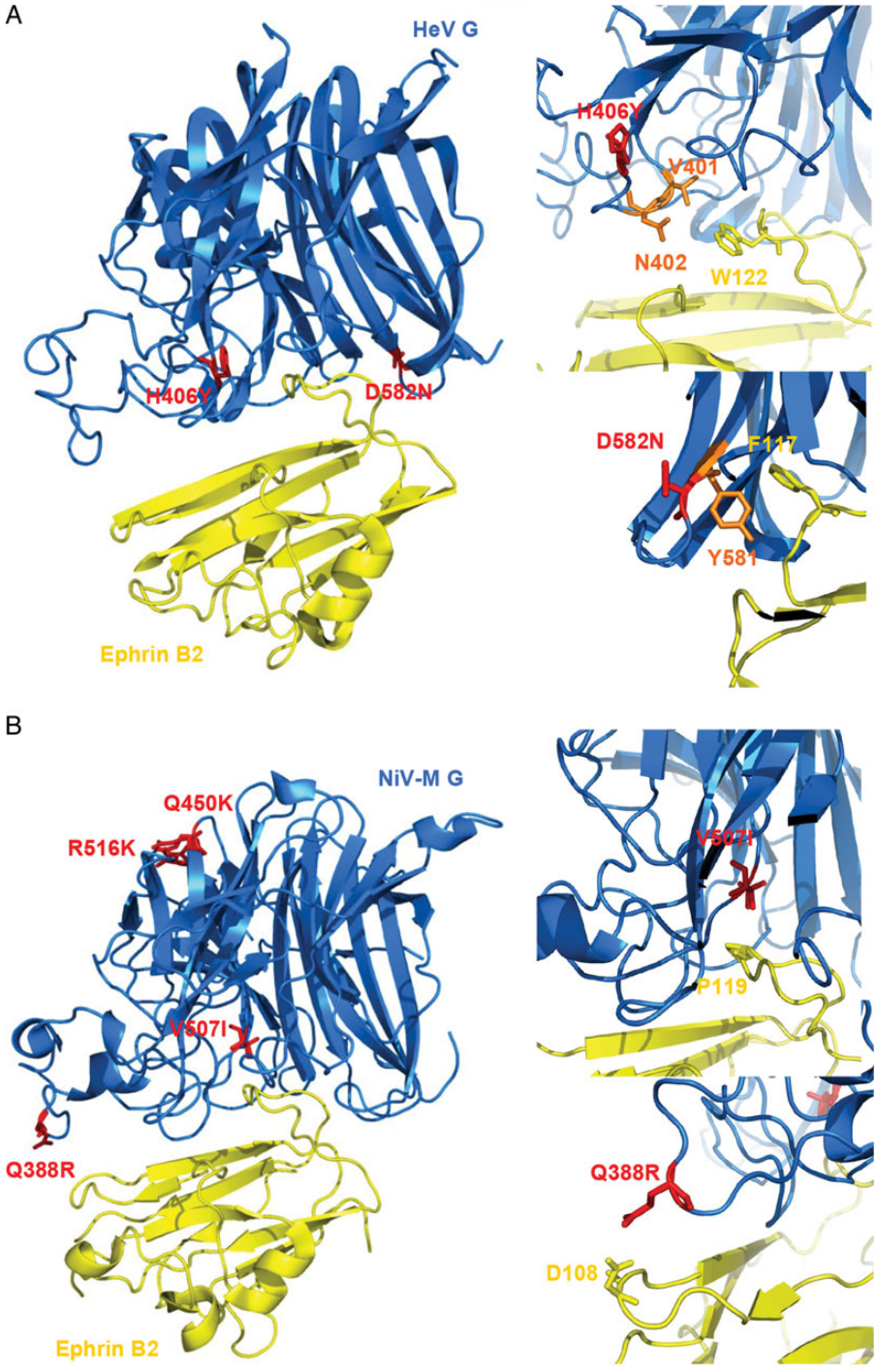

Figure 4. Structural mapping of escape mutations on the Hendra virus (HeV) and Nipah virus (NiV) attachment glycoprotein (G). The neutralization-escape mutations H406Y and D582N (*A*) and Q450K, V507I, and R516K (*B*) were mapped onto the structures of the HeV (*A*) and NiV strain Malaysia (NiV-M; *B*) attachment Gs (in blue), respectively. The changed amino acid residues are shown in red. The structure of ephrin B2 is shown in yellow. Residues involved in the interaction of G and ephrin B2 are shown as sticks in orange (on G) and yellow (on ephrin B2).

with escape from neutralization, did not significantly affect virulence in hamsters. The majority of animals succumbed to disease around day 6 and 7 (Figure 6*A*). Interestingly, animals challenged with the D582N mutant had a slight delay in time to death of 8–9 days, and 1 of 5 animals survived (Figure 6*C*).

While in vitro fitness was not affected by mutations in NiV G that were associated with neutralization escape, these same mutations did significantly affect the virulence in hamsters. Hamsters infected with WT NiV-M succumbed to infection by 3–4 days after challenge (Figure 6*B*). Interestingly, escape

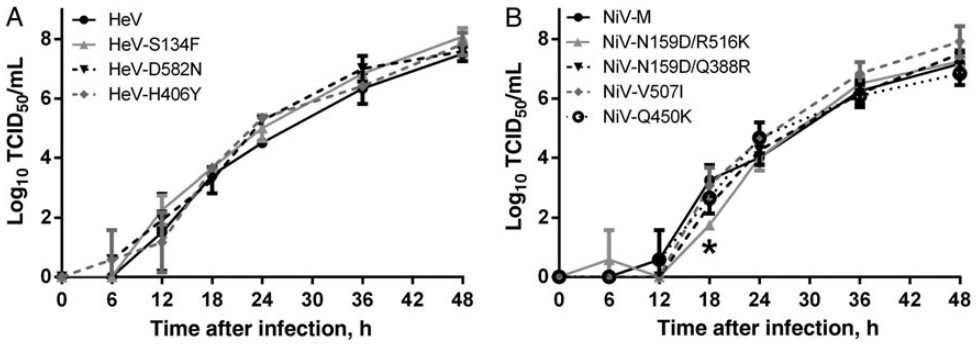

Figure 5. In vitro growth characteristics of wild-type Nipah virus (NiV) and Hendra virus (HeV) and neutralization-escape mutants. Cultures of Vero E6 were infected in triplicate with wild-type and neutralization-escape mutants of HeV (*A*) and NiV strain Malaysia (NiV-M; *B*) at a multiplicity of 0.01, as described in "Materials and Methods" section. Virus titers at different time points were determined by a 50% tissue infective culture dose ($TCID_{50}$) assay, using Vero E6 cells. Error bars represent standard deviations. **P* < .05 by 2-way analysis of variance, compared with the wild-type strain.

mutants with amino acid changes at positions Q388R, Q450K, or V507I were uniformly lethal but showed a significant delay in their time to death by 8–10 days (Figure 6*B* and 6*D*).

Infection of hamsters with WT HeV and NiV resulted in systemic replication of the virus, as previously shown [16]. Infectious HeV and NiV could be detected in brain, lung, spleen, and kidney, and all animals had evidence of viremia on day 3 after infection (data not shown). Once animals were moribund, HeV dissemination of neutralization-escape mutants was similar to that of the WT strain, with the exception of the D582N mutation, which resulted in lack of dissemination in tissues on day 3 and a complete lack of detectable virus replication in the lung (Figure 7*A*). In addition, animals infected with the H406Y mutant had significantly lower levels of virus in the brain

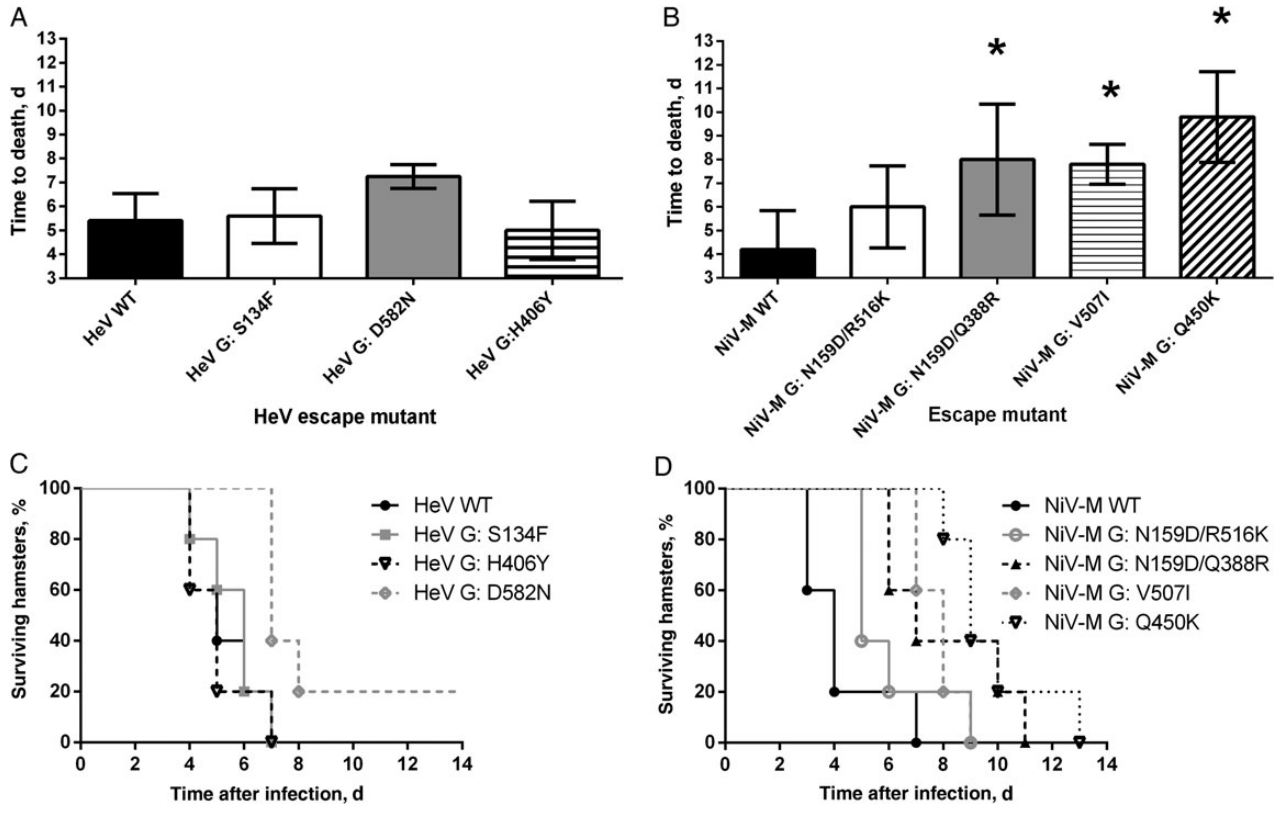

Figure 6. Effect of neutralization escape on virulence of henipaviruses in hamsters. Time to death (*A* and *B*) and percentage survival over time (*C* and *D*) for hamsters infected with wild-type (WT) and neutralization-escape mutants of Hendra virus (HeV; *A* and *C*) and Nipah virus strain Malaysia (NiV-M; *B* and *D*). Error bars represent standard deviations. **P* < .05 by 2-way analysis of variance, compared with the WT strain.

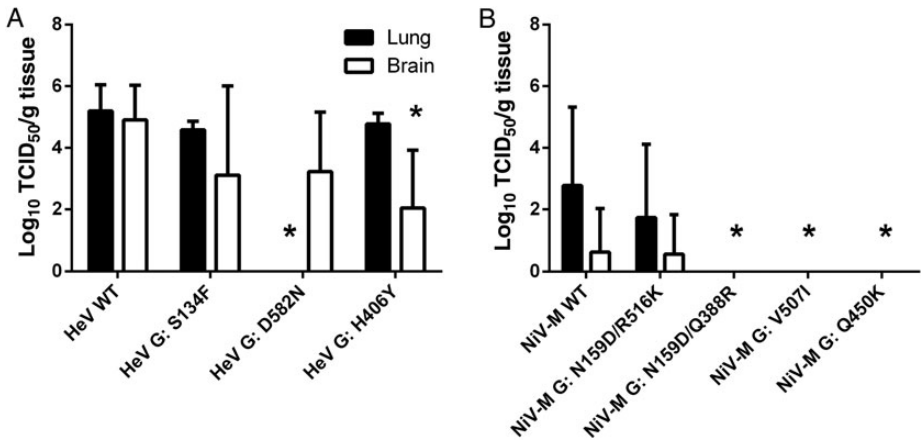

Figure 7. Effect of neutralization escape on replication of henipaviruses in hamsters. Lung (black bar) and brain (white bar) titer results for hamsters infected with wild-type (WT) and neutralization-escape mutants of Hendra virus (HeV; *A*) and Nipah virus strain Malaysia (NiV-M; *B*) when moribund. Lung and brain tissues were harvested from infected hamsters when moribund and were assayed for infectious virus as described in "Materials and Methods" section. Tissue samples from 5 animals were analyzed. Error bars represent standard deviations. *$P < .05$ by 2-way analysis of variance, compared with the WT strain.

(Figure 7*A*). Mutations in the NiV-M G at residues Q388R, V507I, and Q450K resulted in replication below the levels of detection in lungs and brains of moribund hamsters (Figure 7*B*). The mutation at R516K resulted in levels of replication in lungs and brains similar to those for WT NiV-M (Figure 7*B*).

DISCUSSION

We performed a detailed analysis of the residues critical for HNV neutralization by 6 different mAbs. We focused on the G, since this is a major surface membrane glycoprotein that is required for virus attachment and fusion. As previously reported, mAb m102.4 effectively neutralizes HeV and NiV-M, as well as the NiV-B strain [12]. Surprisingly, while the mAb 213 efficiently neutralized the NiV-M strain, the NiV-B strain was not completely neutralized. There are 25 amino acid changes between the G of NiV-M and NiV-B; however, a mutation at residue Q388, which was associated with escape from neutralization by mAb 213, is not one of them. Interestingly, 2 mutations, at residues T385A and K386E, are present in NiV-B, which could affect the structure of the loop responsible for the interaction of Q388 with D108 on the ephrin B2 molecule [18, 19]. It has previously been shown that mAb 213 recognizes a conformational epitope on the NiV-M G and that binding is affected by a N-glycosylation site in the stalk region [20].

All neutralization-escape mutations identified in this study were detected in the HNV G, and no mutations were present in F. This is not surprising, since the mAbs used in this study all targeted the HNV G. Two neutralization-escape mutants had 2 amino acid changes in NiV-M. They shared a mutation at residue N159, but this mutation was unlikely to play a role in neutralization escape, since each escape mutant was only refractory to neutralization by its respective mAb. This suggests that the unique changes at R516K or Q388R and not the common residue at N159D play a role in neutralization escape from mAbs 213 and nAH1.3. The function of the N159D change in association with neutralization escape remains unknown, but it is possible that this is a compensatory change. Position 159 is between 2 critical cysteines, C158 and C162, of the NiV G stalk region that mediate covalent subunit dimerization [21]. Residue 159 is also a predicted glycosylation site (G2) that plays a crucial role in membrane fusion and F triggering [20].

Four of 7 residues associated with escape from neutralization were near or within the receptor-binding domain located on the HNV G. The V507I and D582N mutations in NiV-M and HeV respectively have previously been shown to disrupt m102.4 binding while maintaining high affinity for ephrin B2 and B3. The crystal structure of m102.3 (m102.4 derivative) bound to the HeV G shows that m102.3 resembles the G-H loop of ephrin B2 in both its shape and insertion angle into the HeV G binding pocket [12]. The HeV escape mutant H406Y is adjacent to another binding pocket on the HeV G that is responsible for interacting with the ephrin B2 residue W122 [17]. Finally, the Q388R mutation affects the hydrogen bond between Q388 and D108 on NiV-M G and ephrin B2, respectively [18], which imparts affinity and stabilizes the receptor-bound complex [22]. This hydrogen bond is involved in an area that contains salt bridges and other hydrogen bonds. The Q388R mutation is close to the T385A and K386E found on the NiV-B strain, which could explain why the NiV-B strain is not efficiently neutralized by mAb 213. Interestingly, this epitope is also missing in a recently described HNV isolated from a Ghanaian bat, suggesting that this virus would not be susceptible to neutralization by mAb 213 [22, 23].

It should be noted that the neutralization-escape mutants in the current study were generated under artificial conditions. Since viral proteins can undergo conformational changes under different physiological conditions, the ability or kinetics by

which a mAb binds G can be dependent on the environment [24]. This could potentially affect the escape variants that arise, and therefore it would be interesting compare neutralization-escape mutants that were generated in vitro with those generated in vivo.

We have previously shown that escape from neutralization can be associated with reduced viral fitness [25]. Several neutralization-escape mutations in the receptor-binding domain of SARS coronavirus resulted in reduced replication in a variety of cells and reduced virulence in mice [25]. In the current study, several amino acids associated with neutralization escape were previously shown to be directly involved in binding to the receptor ephrin B2. In a more recent study, we have shown that mutations at V507 and D582 on the NiV-M and HeV G, respectively, did not result in significant differences in replication in vitro [12]. Here we expanded this finding by testing the in vitro replication of 5 other neutralization-escape mutants. Although at least 2 of these mutations were located within the receptor-binding domain, no changes in propagation were detected, but a change at R516K resulted in a lower titer at 18 hours after infection, suggesting that entry may have been affected by this mutation. While virus replication was not affected in cell culture, significant attenuation was observed for some mutants in the hamster model. Several neutralization-escape mutations in NiV-M G resulted in a significant delay in time to death (4–6 days). In addition, a reduction in virus titers was observed in lung and brain tissues, considered key target organs for HNV infection in hamsters [16].

The development of neutralization-escape mutants that are not affected in their in vitro and in vivo replication is a potential concern for the further development of neutralizing mAbs for treatment or prophylaxis. However, treatment of nonhuman primates with m102.4 up to 5 days after infection has completely protected against lethal infection with NiV-M or HeV, and no evidence has been found for the emergence of a neutralization-escape mutant in this model [6, 26].

In conclusion, we have characterized several mAbs that recognize distinct epitopes on the HNV G. Several of these mAbs target epitopes that are directly involved in receptor binding and thus likely inhibit this crucial first step of virus infection. A cocktail of these mAbs may be preferential to a single mAb, given the fact that escape from neutralization can occur without affecting virulence.

Supplementary Data

Supplementary materials are available at http://jid.oxfordjournals.org. Consisting of data provided by the author to benefit the reader, the posted materials are not copyedited and are the sole responsibility of the author, so questions or comments should be addressed to the author.

Notes

Financial support. This work was supported by the Department of Pathology and Institute for Human Infections and Immunity, University of Texas Medical Branch (to B. R.); the Intramural Research Program, National Institute of Allergy and Infectious Diseases, National Institutes of Health (NIH); and the NIH, Department of Health and Human Services (grant AI054715 to C. C. B.).

Potential conflicts of interest. All authors: No reported conflicts. All authors have submitted the ICMJE Form for Disclosure of Potential Conflicts of Interest. Conflicts that the editors consider relevant to the content of the manuscript have been disclosed.

References

1. Rockx B, Winegar R, Freiberg AN. Recent progress in henipavirus research: molecular biology, genetic diversity, animal models. Antiviral Res **2012**; 95:135–49.
2. Marsh GA, de Jong C, Barr JA, et al. Cedar virus: a novel Henipavirus isolated from Australian bats. PLoS Pathog **2012**; 8:e1002836.
3. Guillaume V, Wong KT, Looi RY, et al. Acute Hendra virus infection: analysis of the pathogenesis and passive antibody protection in the hamster model. Virology **2009**; 387:459–65.
4. Bossart KN, Zhu Z, Middleton D, et al. A neutralizing human monoclonal antibody protects against lethal disease in a new ferret model of acute Nipah virus infection. PLoS Pathog **2009**; 5:e1000642.
5. Guillaume V, Contamin H, Loth P, et al. Nipah virus: vaccination and passive protection studies in a hamster model. J Virol **2004**; 78:834–40.
6. Bossart KN, Geisbert TW, Feldmann H, et al. A neutralizing human monoclonal antibody protects African green monkeys from Hendra virus challenge. Sci Transl Med **2011**; 3:105ra3.
7. Bossart KN, Rockx B, Feldmann F, et al. A Hendra virus G glycoprotein subunit vaccine protects African green monkeys from Nipah virus challenge. Sci Transl Med **2012**; 4:146ra07.
8. Zhu Z, Dimitrov AS, Bossart KN, et al. Potent neutralization of Hendra and Nipah viruses by human monoclonal antibodies. J Virol **2006**; 80:891–9.
9. Johnson JB, Aguilar HC, Lee B, Parks GD. Interactions of human complement with virus particles containing the Nipah virus glycoproteins. J Virol **2011**; 85:5940–8.
10. Aguilar HC, Ataman ZA, Aspericueta V, et al. A novel receptor-induced activation site in the Nipah virus attachment glycoprotein (G) involved in triggering the fusion glycoprotein (F). J Biol Chem **2009**; 284:1628–35.
11. Smith EC, Popa A, Chang A, Masante C, Dutch RE. Viral entry mechanisms: the increasing diversity of paramyxovirus entry. FEBS J **2009**; 276:7217–27.
12. Xu K, Rockx B, Xie Y, et al. Crystal structure of the Hendra virus attachment G glycoprotein bound to a potent cross-reactive neutralizing human monoclonal antibody. PLoS Pathog **2013**; 9:e1003684.
13. Escaffre O, Borisevich V, Carmical JR, et al. Henipavirus pathogenesis in human respiratory epithelial cells. J Virol **2013**; 87:3284–94.
14. Zhu Z, Bossart KN, Bishop KA, et al. Exceptionally potent cross-reactive neutralization of Nipah and Hendra viruses by a human monoclonal antibody. J Infect Dis **2008**; 197:846–53.
15. Bowden TA, Aricescu AR, Gilbert RJ, Grimes JM, Jones EY, Stuart DI. Structural basis of Nipah and Hendra virus attachment to their cell-surface receptor ephrin-B2. Nat Struct Mol Biol **2008**; 15:567–72.
16. Rockx B, Brining D, Kramer J, et al. Clinical outcome of henipavirus infection in hamsters is determined by the route and dose of infection. J Virol **2011**; 85: 7658–71.
17. Xu K, Chan YP, Rajashankar KR, et al. New insights into the Hendra virus attachment and entry process from structures of the virus G glycoprotein and its complex with ephrin-B2. PLoS One **2012**; 7.
18. Xu K, Rajashankar KR, Chan YP, Himanen JP, Broder CC, Nikolov DB. Host cell recognition by the henipaviruses: crystal structures of the Nipah G attachment glycoprotein and its complex with ephrin-B3. Proc Natl Acad Sci U S A **2008**; 105:9953–8.
19. Harcourt BH, Lowe L, Tamin A, et al. Genetic characterization of Nipah virus, Bangladesh, 2004. Emerg Infect Dis **2005**; 11:1594–7.
20. Biering SB, Huang A, Vu AT, et al. N-Glycans on the Nipah virus attachment glycoprotein modulate fusion and viral entry as they protect against antibody neutralization. J Virol **2012**; 86:11991–2002.
21. Maar D, Harmon B, Chu D, et al. Cysteines in the stalk of the Nipah virus G glycoprotein are located in a distinct subdomain critical for fusion activation. J Virol **2012**; 86:6632–42.
22. Lee B, Pernet O, Ahmed AA, Zeltina A, Beaty SM, Bowden TA. Molecular recognition of human ephrinB2 cell surface receptor by an emergent African henipavirus. Proc Natl Acad Sci U S A **2015**; 112:E2156–65.
23. Drexler JF, Corman VM, Muller MA, et al. Bats host major mammalian paramyxoviruses. Nat Commun **2012**; 3:796.
24. Witz J, Brown F. Structural dynamics, an intrinsic property of viral capsids. Arch Virol **2001**; 146:2263–74.
25. Rockx B, Donaldson E, Frieman M, et al. Escape from human monoclonal antibody neutralization affects in vitro and in vivo fitness of severe acute respiratory syndrome coronavirus. J Infect Dis **2010**; 201:946–55.
26. Geisbert TW, Mire CE, Geisbert JB, et al. Therapeutic treatment of Nipah virus infection in nonhuman primates with a neutralizing human monoclonal antibody. Sci Transl Med **2014**; 6:242ra82.